Forces in Mechanics 7 (2022) 100091

Contents lists available at ScienceDirect

Forces in Mechanics

journal homepage: www.sciencedirect.com/journal/forces-in-mechanics

# On the effective property of a micro-cracked and a microscopically curved interface between dissimilar materials

Hui Fan [a], Whye-Teong Ang [*,a], Xue Wang [a,1]

[a] School of Mechanical and Aerospace Engineering, Nanyang Technological University, Singapore

ARTICLE INFO

*Keywords:*
Micromechanics
Imperfect interfaces
Micro-cracked interface
Wavy interface
Effective properties
Boundary integral equations

ABSTRACT

Two different types of imperfect interfaces between dissimilar elastic materials under antiplane deformations are studied using micromechanics concepts. Interfaces containing interfacial micro-cracks and those that are microscopically wavy (sinusoidal) are modeled as spring-like and membrane-like respectively at the macroscopic level. The strain energy in the microscopic configuration is equated to that in the macroscopic configuration in order to estimate the effective properties of the imperfect interfaces. The boundary value problems for computing the strain energy at the microscopic level are formulated and solved by using boundary integral equations.

## 1. Introduction

Since the 1970s, the continuum mechanics approach based on the works of Gurtin and Murdoch [1,2] has been widely used for analyzing interfaces between solids. In such an approach, the interface is modeled as an elastic membrane with residual strain and with elastic constants that are different from the bulk materials. Another approach which uses asymptotic analysis on equations of elasticity in a very thin elastic layer between two elastic materials to derive different types of interface conditions is given in Benveniste and Miloh [3]. The conditions derived in [3] for a stiffened interface may be shown to be consistent with the membrane interfacial conditions in [1,2] and [4].

Micromechanical models may be developed to provide a link between interfacial micro-structures and the macro-scale (continuum) effective properties of interfaces (see, for example, Fan and Sze [5]). They (the models) may also be used to validate physically the existence of the different types of interfaces derived in [1,4].

Two different types of imperfect interfaces between dissimilar elastic materials under antiplane deformations are studied in the current paper. Specifically, of interest here is the estimation of the effective property of a microscopically damaged and a microscopically curved interface. The microscopically damaged interface between two dissimilar materials is modeled as containing a periodic array of interfacial micro-cracks, as in Wang et al [6,7]. The micro-cracked interface is modeled as spring-like at the macroscopic level. The microscopically curved interface has a wavy (sinusoidal) profile, as in Fan and Xiao [8]. The microscopically wavy interface is modeled as flat and membrane-like at the macroscopic level.

As shown in [5,6] and [7], the effective property of the micro-cracked interface may be estimated by averaging the displacement jump across the micro-cracks and the normal stress on the interface. Such an averaging procedure leads to indeterminacy, however, when it is applied to estimate the effective property of the microscopically wavy interface.

An alternative approach based on energy consideration is proposed here for estimating effective properties of the interfaces. The strain energy in the microscopic configuration is equated to that in the macroscopic configuration in order to estimate the effective properties of the imperfect interfaces. The boundary value problems for computing the strain energy at the microscopic level are formulated and solved by using boundary integral equations.

The effective property of the interface damaged by the periodically distributed interfacial micro-cracks as obtained via the energy approach is numerically found to agree closely with that computed by using the averaging procedure in [5,6] and [7]. For the microscopically wavy interface, we use the energy approach to investigate the effects of the wavy interface amplitude and the shear moduli of the materials on the effective property of the interface.

* Corresponding author.
*E-mail address:* mwtang@ntu.edu.sg (W.-T. Ang).
[1] Current affiliation: Singapore Research Center, TE Connectivity

https://doi.org/10.1016/j.finmec.2022.100091
Received 16 January 2022; Received in revised form 7 February 2022; Accepted 6 March 2022
Available online 8 March 2022

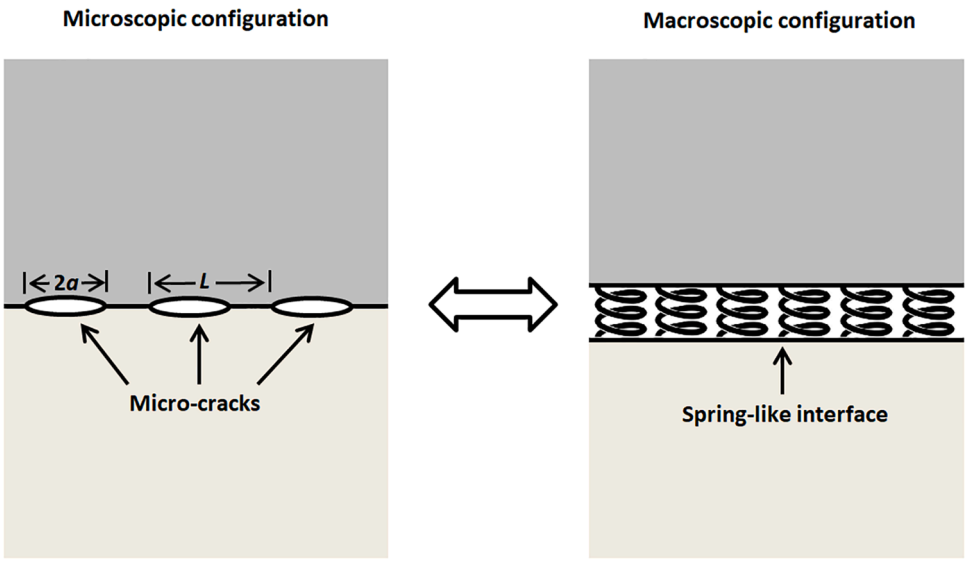


**Fig. 1.** The micro-cracked and the spring-like interfaces.

## 2. Macroscopic boundary conditions for the spring-like and membrane-like interfaces

With reference to a Cartesian coordinate system $Ox_1x_2x_3$, consider two dissimilar isotropic elastic materials occupying the half-spaces $x_2 > 0$ and $x_2 < 0$. The bimaterial is assumed to undergo an antiplane deformation such that the only non-zero component of the displacement is in the $x_3$ direction and given by the function $w(x_1, x_2)$. The only non-zero components of the stress are given by

$$\sigma_{k3} = \sigma_{3k} = \begin{cases} \mu^{(1)} \dfrac{\partial w}{\partial x_k} & \text{for} \quad x_2 > 0 \\ \mu^{(2)} \dfrac{\partial w}{\partial x_k} & \text{for} \quad x_2 < 0 \end{cases} \qquad (k = 1, 2), \tag{1}$$

where $\mu^{(1)}$ and $\mu^{(2)}$ are the constant shear moduli of the materials in the half-spaces.

For the antiplane deformation, three different types of conditions may be derived for the interface $x_2 = 0$ between the elastic materials in the half-spaces $x_2 > 0$ and $x_2 < 0$, as in Benveniste and Miloh [3]. They are:

$$\left.\begin{array}{rcl} \sigma_{32}(x_1, 0^+) & = & \sigma_{32}(x_1, 0^-) \\ K\Delta w(x_1) & = & \sigma_{32}(x_1, 0) \end{array}\right\} \text{ softened or spring-like interface,} \tag{2}$$

$$\left.\begin{array}{rcl} w(x_1, 0^+) & = & w(x_1, 0^-) \\ \sigma_{32}(x_1, 0^+) & = & \sigma_{32}(x_1, 0^-)) \end{array}\right\} \text{ ideal or perfectly bonded interface,} \tag{3}$$

$$\left.\begin{array}{rcl} w(x_1, 0^+) & = & w(x_1, 0^-) \\ \Delta\sigma_{32}(x_1) & = & -\mu_s \dfrac{d^2}{dx_1^2}(w(x_1, 0)) \end{array}\right\} \text{ stiffened or membrane-like interface,} \tag{4}$$

where $\Delta w(x_1) = w(x_1, 0^+) - w(x_1, 0^-)$, $\Delta\sigma_{32}(x_1) = \sigma_{32}(x_1, 0^+) - \sigma_{32}(x_1, 0^-)$, $K$ is the interface spring constant of the softened interface, and the constant $\mu_s$, as we shall see, may be interpreted as the interface membrane shear modulus defined in the theory of surface elasticity of Gurtin et al [1,2] and [4].

In Benveniste and Miloh [3], the interface conditions above are derived by performing asymptotic analysis on the equations of elasticity in a thin elastic layer $-\delta < x_2 < \delta$ between two elastic half-spaces $x_2 > \delta$ and $x_2 < -\delta$, for small $\delta$. The conditions in (2) and (4) are obtained by taking the shear modulus in the layer to be proportional in magnitude to $\delta$ and $1/\delta$ respectively and by letting $\delta$ tend to zero. As we show below, the conditions in (4) for the stiffened interface may also be derived from the equations of surface elasticity.

The surface elasticity equations on the flat interface $x_2 = 0$ under a general deformation are given by (see equation (4) in Gurtin and Murdoch [2])

$$\Delta\sigma_{i2}(x_1) + \frac{\partial \Sigma_{i\beta}}{\partial x_\beta} = 0 \tag{5}$$

and

$$\begin{aligned} \Sigma_{\alpha\beta} &= \sigma_0\delta_{\alpha\beta} + (\mu_s - \sigma_0)\left(\frac{\partial u_\alpha}{\partial x_\beta} + \frac{\partial u_\beta}{\partial x_\alpha}\right) + (\lambda_s + \sigma_0)\frac{\partial u_\gamma}{\partial x_\gamma}\delta_{\alpha\beta} + \sigma_0\frac{\partial u_\alpha}{\partial x_\beta}, \\ \Sigma_{2\beta} &= \sigma_0\frac{\partial u_2}{\partial x_\beta}, \end{aligned} \tag{6}$$

where Greek subscripts have values 1 and 3 only while Latin subscripts have values 1, 2 and 3 in the equations above, $\Delta\sigma_{i2}(x_1)$ denotes the jump in $\sigma_{i2}$ across opposite sides of the interface, $\Sigma_{i\beta}$ is the surface stress tensor, $\delta_{\alpha\beta}$ is the Kronecker-delta, $(u_1, u_2, u_3)$ is the displacement on the interface, $\sigma_0$ is the surface tension and $\lambda_s$ and $\mu_s$ are the surface Lame constants. Note that the Einstenian convention of summing over repeated indices applies for both Greek and Latin subscripts in (5) and (6).

For antiplane deformation, $u_1 = u_2 = 0$ and $u_3$ is a function of $x_1$ only. Thus, we may reduce (5) and (6) respectively to

$$\Delta\sigma_{32}(x_1) + \frac{d\Sigma_{31}}{dx_1} = 0, \tag{7}$$

and

$$\Sigma_{31} = \mu_s\frac{du_3}{dx_1}. \tag{8}$$

The condition for the normal stress jump across a stiffened interface in (4) (as given in [3]) is recovered if (8) is substituted into (7) and if the interface displacement $u_3$ matches the antiplane bulk displacement $w$ (that is, $u_3(x_1) = w(x_1, 0^+) = w(x_1, 0^-)$).

Interfaces damaged by interfacial micro-cracks and those that are microscopically curved may be modeled as spring-like and membrane-like interfaces respectively at the macroscopic level. The effects of the

interfacial micro-cracks and the interfacial curvature at the microscopical level are respectively captured in the coefficients $K$ and $\mu_s$ in (2) and (4). We refer to $K$ and $\mu_s$ as the effective properties of the micro-cracked and the microscopically curved interfaces respectively.

## 3. A microscopically damaged interface

### 3.1. Microscopic and macroscopic models

At the microscopic level, the bimaterial interface at $x_2 = 0$ is modeled as having a periodic array of evenly spaced out equal length micro-cracks in the regions $-a + nL < x_1 < a + nL$, $x_2 = 0$, for $n = 0, \pm 1, \pm 2, \cdots$, where $a$ and $L$ are positive constants such that $2a < L$. The parts of the interface outside the interfacial micro-cracks are perfectly bonded. The interface is characterized by the half length $a$ of the micro-crack and the micro-crack density $\rho = 2a/L$. At the macroscopic level, the micro-cracked interface is modeled as a spring-like interface which satisfies the interfacial conditions in (2), as the micro-cracks give rise to a displacement jump across the interface. A sketch of the micro-cracked and the spring-like interfaces is given in Fig. 1.

Given the shear moduli $\mu^{(1)}$ and $\mu^{(2)}$ and the parameters $a$ and $\rho$ which characterize the micro-model of the interface, we are interested in estimating the effective property $K$ of the micro-cracked interface.

### 3.2. Estimation of effective property

To estimate the effective property $K$, let the antiplane stress throughout the whole bimaterial with the periodic array of interfacial micro-cracks be given by

$$\sigma_{3k}(x_1, x_2) = S_0\delta_{k2} + \sigma_{3k}^{(\mathrm{cr})}(x_1, x_2), \tag{9}$$

where $S_0$ is the uniform load on the bimaterial and $\sigma_{3k}^{(\mathrm{cr})}$ are the antiplane stresses induced by the presence of the interfacial micro-cracks, that is, $\sigma_{3k}^{(\mathrm{cr})}(x_1, x_2) = 0$ in the bimaterial if the interface does not contain any micro-cracks. Henceforth, all Latin subscripts are assume to run from 1 to 2 only.

The stresses $\sigma_{3k}^{(\mathrm{cr})}$ at any interior point $(\xi_1, \xi_2)$ are given by the boundary integral equation

$$\begin{aligned}\sigma_{3k}^{(\mathrm{cr})}(\xi_1, \xi_2) &= \frac{\mu^{(1)}\mu^{(2)}}{\pi(\mu^{(1)} + \mu^{(2)})}\int_{-a}^{a} \Delta w^{(\mathrm{cr})}(x_1)(\delta_{2k} - i\delta_{1k}) \\ &\quad \times \mathrm{Re}\left\{\frac{1}{(x_1 - \xi_1 - i\xi_2)^2} + \Theta(x_1, \xi_1 + i\xi_2)\right\} dx_1,\end{aligned} \tag{10}$$

where $\Delta w^{(\mathrm{cr})}(x_1)$ is the antiplane displacement jump across the micro-cracks and $\Theta(x_1, z)$ is defined by

$$\Theta(x_1, z) = \frac{1}{L^2}\Psi_1\left(\frac{L + x_1 - z}{2}\right) + \frac{1}{L^2}\Psi_1\left(\frac{L + z - x_1}{2}\right), \tag{11}$$

**Table 1**
A comparison of the numerical values of $a(\mu^{(1)} + \mu^{(2)})K/(2\mu^{(1)}\mu^{(2)})$ obtained by the strain energy approach and the averaging procedure.

| Micro-crack density $\rho$ | Strain energy approach | Finite element model in [5] |
|---|---|---|
| 0.05 | 12.72 | 13.37 |
| 0.10 | 6.364 | 6.494 |
| 0.20 | 3.138 | 3.175 |
| 0.30 | 2.045 | 2.048 |
| 0.40 | 1.484 | 1.473 |
| 0.50 | 1.134 | 1.111 |
| 0.60 | 0.8877 | 0.8571 |
| 0.70 | 0.6969 | 0.6542 |
| 0.80 | 0.5356 | 0.4819 |
| 0.90 | 0.3815 | 0.3125 |

with $\Psi_1(z)$ being the trigamma function. Note that $z$ is in general a complex variable. The integration in (10) is over only the micro-crack in the region $-a < x_1 < a$, $x_2 = 0$.

The micro-cracks are traction free, that is, $\sigma_{32}^{(\mathrm{cr})} = -S_0$ on the micro-cracks. Together with (10), this gives rise to the hypersingular integral equation

$$\begin{aligned}\mathscr{H}\int_{-a}^{a} \frac{\Delta w^{(\mathrm{cr})}(x_1)}{(x_1 - \xi_1)^2} dx_1 + \int_{-a}^{a} \Delta w^{(\mathrm{cr})}(x_1)\Theta(x_1, \xi_1) dx_1 &= -\pi\left(\frac{1}{\mu^{(1)}} + \frac{1}{\mu^{(2)}}\right) S_0 \\ &\text{for } -a < \xi_1 < a,\end{aligned} \tag{12}$$

where $\mathscr{H}\int$ denotes that the integral is to be interpreted in the Hadamard finite-part sense. Details on the derivations of (10) and (12) are given in Wang et al [6].

The hypersingular integral equation in (12) may be solved for $\Delta w^{(\mathrm{cr})}(x_1)$ by using approximate techniques in Ang [9] and Kaya and Erdogan [10]. Once the hypersingular integral equation in (12) is solved for the displacement jump $\Delta w^{(\mathrm{cr})}(x_1)$, the effective property $K$ may be readily computed from

$$\frac{K}{L}\int_{-a}^{a} \Delta w^{(\mathrm{cr})}(x_1) dx_1 = S_0. \tag{13}$$

The formula in (13) is obtained from (2) by using the average values of the displacement jump and the traction over a period length of the micro-cracked interface. Such an averaging procedure is used in Wang et al [6]-[7] for computing $K$.

An alternative approach based on strain energy consideration is proposed here for estimating the effective property $K$. To obtain a formula for $K$, the total strain energy of the bimaterial in the microscopic (periodic interfacial crack) model (as calculated by using the stress field in (9)) is equated to the corresponding strain energy in the bimaterial with the macroscopic (spring-like) model of the interface.

From (9), the total strain energy in the representative region $-L/2 < x_1 < L/2$, $-\infty < x_2 < \infty$, $0 < x_3 < B$, of the bimaterial with the micro-cracked interface is given by

$$\begin{aligned}U^{(\mathrm{micro})} &= \frac{1}{2}\lim_{H\to\infty}\int_0^B\int_{-H}^{H}\int_{-L/2}^{L/2} 2\sigma_{3k}\varepsilon_{3k} dx_1 dx_2 dx_3 \\ &= \frac{B}{2}\lim_{H\to\infty}\int_{-H}^{H}\int_{-L/2}^{L/2}\frac{1}{\mu}\sigma_{3k}\sigma_{3k} dx_1 dx_2 \\ &= \frac{B}{2}S_0^2 L\left(\frac{1}{\mu^{(1)}} + \frac{1}{\mu^{(2)}}\right)\lim_{H\to\infty} H \\ &\quad + \frac{B}{2}\int_{-\infty}^{\infty}\int_{-L/2}^{L/2}\frac{1}{\mu}\left(2S_0\sigma_{32}^{(\mathrm{cr})} + \sigma_{3k}^{(\mathrm{cr})}\sigma_{3k}^{(\mathrm{cr})}\right) dx_1 dx_2.\end{aligned} \tag{14}$$

Note that $\mu$ is given by $\mu^{(1)}$ for $x_2 > 0$ and by $\mu^{(2)}$ for $x_2 < 0$.

The corresponding total strain energy in the bimaterial with the spring-like interface governed by (2) is given by

$$\begin{aligned}U^{(\mathrm{macro})} &= \frac{B}{2}\lim_{H\to\infty}\int_{-H}^{H}\int_{-L/2}^{L/2}\frac{1}{\mu}S_0^2 dx_1 dx_2 + \frac{B}{2}\int_{-L/2}^{L/2} S_0\Delta w(x_1) dx_1 \\ &= \frac{B}{2}S_0^2 L\left(\frac{1}{\mu^{(1)}} + \frac{1}{\mu^{(2)}}\right)\lim_{H\to\infty} H + \frac{BLS_0^2}{2K}.\end{aligned} \tag{15}$$

Setting $U^{(\mathrm{micro})} = U^{(\mathrm{macro})}$ yields the formula

$$K = L\left(\int_{-\infty}^{\infty}\int_{-L/2}^{L/2}\frac{1}{\mu}\left(2\frac{\sigma_{32}^{(\mathrm{cr})}}{S_0} + \frac{\sigma_{3k}^{(\mathrm{cr})}\sigma_{3k}^{(\mathrm{cr})}}{S_0^2}\right) dx_1 dx_2\right)^{-1}. \tag{16}$$

Once the hypersingular integral equation in (12) is solved for the displacement jump $\Delta w^{(\mathrm{cr})}(x_1)$, the stresses $\sigma_{3k}^{(\mathrm{cr})}$ may be computing at any point in the interior of the bimaterial by using the integral formula in (10). The double integral in (12) may be evaluated numerically by

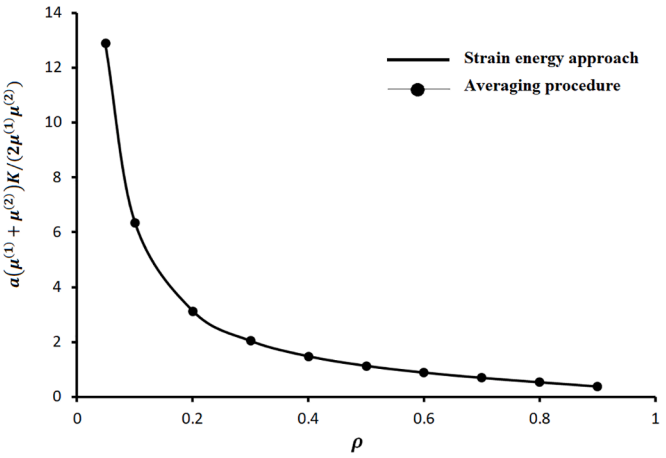


**Fig. 2.** Plots of $a(\mu^{(1)}+\mu^{(2)})K/(2\mu^{(1)}\mu^{(2)})$ against $\rho$.

replacing the integration domain $-L/2 < x_1 < L/2,\ -\infty < x_2 < \infty$, with $-L/2 < x_1 < L/2,\ -H < x_2 < H$, where $H$ is a sufficiently large positive real number, and by partitioning the truncated region of integration into many small rectangular cells.

### 3.3. Results

The non-dimensionalized effective property $a(\mu^{(1)}+\mu^{(2)})K/(2\mu^{(1)}\mu^{(2)})$ is a function of only the micro-crack density $\rho$.

In Table 1, for selected values of $\rho$, the numerical values of $a(\mu^{(1)}+\mu^{(2)})K/(2\mu^{(1)}\mu^{(2)})$ obtained by the strain energy approach are compared with those calculated by a finite element method in [5]. The finite element procedure in [5], which is based on a three phase model of the micro-cracked interface, is computationally intensive, requiring as many as ten thousand elements. The two sets of numerical values in Table 1 are quite close to each other. They agree to at least two significant figures for $\rho$ that is less than 0.60. For $\rho$ closer to 1, the difference between the two sets of numerical values is more pronounced probably because of a larger error in the finite element calculation.

Plots of $a(\mu^{(1)}+\mu^{(2)})K/(2\mu^{(1)}\mu^{(2)})$ against $\rho$, obtained using the strain energy approach and the averaging procedure in Wang et al [6]-[7], are compared in Fig. 2. The two plots are almost indistinguishable, showing excellent agreement. The percentage difference in the numerical values of $a(\mu^{(1)}+\mu^{(2)})K/(2\mu^{(1)}\mu^{(2)})$ in the two plots is less than 1%.

Fig. 2 shows that $a(\mu^{(1)}+\mu^{(2)})K/(2\mu^{(1)}\mu^{(2)})$ tends to infinity as the micro-crack density $\rho$ approaches zero. Thus, the effective property $K$ tends to infinity, that is, the interface becomes perfect with zero interfacial displacement jump, as $a$ approaches zero (for a fixed $L$) or as $L$ approaches infinity (for a fixed $a$), as expected.

The comparisons in Table 1 and Fig. 2 validate both the strain energy approach here and the averaging procedure for computing the effective property $K$.

The averaging procedure in [6,7] is much less computationally intensive than the strain energy approach here. However, it cannot be extended to estimate the effective property of the microscopically curved interface considered below.

## 4. A microscopically curved interface

### 4.1. Microscopic and macroscopic models

At the microscopic level, the microscopically curved interface is modeled as having a sinusoidal profile given by $x_2 = A_0\sin(2\pi x_1/h),\ -\infty < x_1 < \infty$, where $A_0$ and $h$ are positive constants. The shear modulus of the material in the region $x_2 > A_0\sin(2\pi x_1/h),\ -\infty < x_1 < \infty$, is given by $\mu^{(1)}$, and that in the region $x_2 < A_0\sin(2\pi x_1/h),\ -\infty < x_1 < \infty$, by $\mu^{(2)}$. The two half-space regions are perfectly bonded. Since the traction $\sigma_{3k}n_k$, where $n_k$ is the $x_k$ component of a unit normal vector to the surface $x_2 = A_0\sin(2\pi x_1/h)$, is continuous across the sinusoidal interface, a jump in the stress component $\sigma_{32}$ exists across the interface. Hence, at the macroscopic level, the sinusoidal interface may be modeled as a plane (flat) membrane-like interface satisfying the interfacial conditions in (4) with a jump in $\sigma_{32}$. A sketch of the wavy and the membrane-like interfaces is given in Fig. 3.

Given the shear moduli $\mu^{(1)}$ and $\mu^{(2)}$ and the parameters $A_0$ and $h$ which characterize the micro-model of the interface, we are interested in estimating the effective property $\mu_s$ of the microscopically wavy interface.

### 4.2. Estimation of effective property

To estimate the effective property $\mu_s$ of the sinusoidal interface, the antiplane strains in the bimaterial are taken to be given by

$$\varepsilon_{3k}(x_1,x_2) = \Gamma_0\delta_{k1} + \varepsilon_{3k}^{(\mathrm{in})}(x_1,x_2), \tag{17}$$

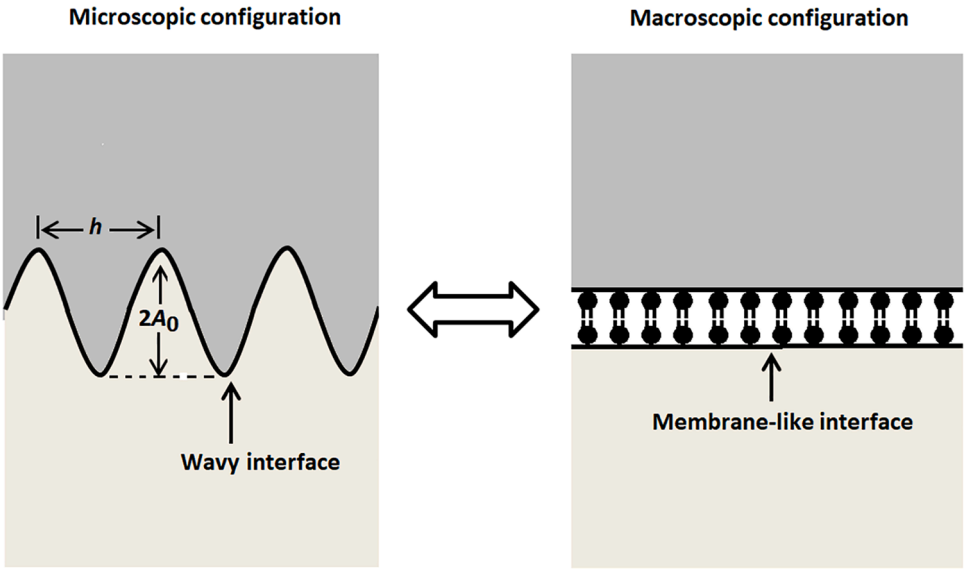


**Fig. 3.** The wavy and the membrane-like interfaces.

where the strains $\varepsilon_{3k}^{(\mathrm{in})}(x_1,x_2)$ are such that $\varepsilon_{3k}^{(\mathrm{in})}(x_1,x_2)=0$ if $A_0=0$ and $\Gamma_0$ is a given constant.

Consider a representative strip of the bimaterial with the sinusoidal interface over a period interval. The strip occupies the region $0<x_1<h,-\infty<x_2<\infty$. Denote the upper half of the strip $x_2>A_0\sin(2\pi x_1/h)$, $0<x_1<h$, by $R^{(1)}$, the lower half $x_2<A_0\sin(2\pi x_1/h)$, $0<x_1<h$, by $R^{(2)}$, and the interface $x_2=A_0\sin(2\pi x_1/h)$, $0<x_1<h$, by $C$.

Let $w^{(r)}$ be the displacement field which gives rise to the strains $\varepsilon_{3k}^{(\mathrm{in})}(x_1,x_2)$ in $R^{(r)}$, that is,

$$\varepsilon_{3k}^{(\mathrm{in})}(x_1,x_2)=\frac{1}{2}\frac{\partial w^{(r)}}{\partial x_k}\ \text{for}\ (x_1,x_2)\in R^{(r)}\ \ (r=1,2). \tag{18}$$

The displacement $w^{(r)}$ satisfies the two-dimensional Laplace's equation in $R^{(r)}$ and is such that the strains $\varepsilon_{3k}^{(r)}$ vanish as $|x_2|$ tends to infinity, and

$$\begin{aligned}&\left.\frac{\partial w^{(1)}}{\partial x_1}\right|_{x_1=0}=0\ \text{and}\left.\frac{\partial w^{(1)}}{\partial x_1}\right|_{x_1=h}=0\ \text{for}\ 0<x_2<\infty,\\&\left.\frac{\partial w^{(2)}}{\partial x_1}\right|_{x_1=0}=0\ \text{and}\left.\frac{\partial w^{(2)}}{\partial x_1}\right|_{x_1=h}=0\ \text{for}\ -\infty<x_2<0.\end{aligned} \tag{19}$$

From (17) and (19), the loads on the edges of the representative strip are given by

$$\begin{aligned}\sigma_{31}(0,x_2)&=2\mu^{(1)}\Gamma_0\ \text{and}\ \sigma_{31}(h,x_2)=2\mu^{(1)}\Gamma_0\ \text{for}\ 0<x_2<\infty,\\\sigma_{31}(0,x_2)&=2\mu^{(2)}\Gamma_0\ \text{and}\ \sigma_{31}(h,x_2)=2\mu^{(2)}\Gamma_0\ \text{for}\ -\infty<x_2<0.\end{aligned} \tag{20}$$

The continuity conditions for the perfectly bonded sinusoidal interface give

$$w^{(1)}=w^{(2)}\ \text{and}\ \mu^{(1)}p^{(1)}-\mu^{(2)}p^{(2)}=2\Gamma_0 n_1\left(\mu^{(2)}-\mu^{(1)}\right)\ \text{for}\ (x_1,x_2)\in C, \tag{21}$$

where $p^{(r)}=n_k\,\partial w^{(r)}/\partial x_k$ and $n_k(x_1,x_2)$ is the $x_k$ component of the unit normal vector at the point $(x_1,x_2)$ on the interface $C$, pointing away from the region $R^{(1)}$.

We derive the boundary integral equations

$$\begin{aligned}\lambda^{(1)}(\xi_1,\xi_2)w^{(1)}(\xi_1,\xi_2)&=\int_C\left(w^{(1)}(x_1,x_2)\Lambda^{(1)}(x_1,x_2;\xi_1,\xi_2)\right.\\&\left.-p^{(1)}(x_1,x_2)\Phi^{(1)}(x_1,x_2;\xi_1,\xi_2)\right)ds(x_1,x_2)\\&\qquad\text{for}\ (x_1,x_2)\in R^{(1)}\cup C,\end{aligned} \tag{22}$$

and

$$\begin{aligned}\lambda^{(2)}(\xi_1,\xi_2)w^{(2)}(\xi_1,\xi_2)&=\int_C\left(-w^{(2)}(x_1,x_2)\Lambda^{(2)}(x_1,x_2;\xi_1,\xi_2)\right.\\&\left.+p^{(2)}(x_1,x_2)\Phi^{(2)}(x_1,x_2;\xi_1,\xi_2)\right)ds(x_1,x_2)\\&\qquad\text{for}\ (x_1,x_2)\in R^{(2)}\cup C,\end{aligned} \tag{23}$$

where $\lambda^{(r)}(\xi_1,\xi_2)$ has the value $1/2$ if $(\xi_1,\xi_2)$ lies on a smooth part of $C$, and the value 1 if $(\xi_1,\xi_2)$ lies in the interior of the region $R^{(r)}$, $p^{(r)}(x_1,x_2)=n_k(x_1,x_2)\partial w^{(r)}/\partial x_k$, $\Lambda^{(r)}=n_k(x_1,x_2)\partial\Phi^{(r)}/\partial x_k$ and $\Phi^{(r)}$ is defined by

$$\begin{aligned}&\Phi^{(r)}(x_1,x_2;\xi_1,\xi_2)\\&=\frac{1}{4\pi}\ln\left(\left(f^{(r)}(x_1,x_2)-f^{(r)}(\xi_1,\xi_2)\right)^2+\left(g^{(r)}(x_1,x_2)-g^{(r)}(\xi_1,\xi_2)\right)^2\right)\\&+\frac{1}{4\pi}\ln\left(\left(f^{(r)}(x_1,x_2)-f^{(r)}(\xi_1,\xi_2)\right)^2+\left(g^{(r)}(x_1,x_2)+g^{(r)}(\xi_1,\xi_2)\right)^2\right),\end{aligned} \tag{24}$$

with the conformal mapping functions $f^{(r)}(x_1,x_2)$ and $g^{(r)}(x_1,x_2)$ given by

$$\begin{aligned}f^{(1)}(x_1,x_2)&=\exp\left(-\frac{\pi x_2}{h}\right)\cos\left(\frac{\pi x_1}{h}\right),\\g^{(1)}(x_1,x_2)&=\exp\left(-\frac{\pi x_2}{h}\right)\sin\left(\frac{\pi x_1}{h}\right),\\f^{(2)}(x_1,x_2)&=\exp\left(\frac{\pi x_2}{h}\right)\cos\left(\frac{\pi x_1}{h}\right),\\g^{(2)}(x_1,x_2)&=-\exp\left(\frac{\pi x_2}{h}\right)\sin\left(\frac{\pi x_1}{h}\right).\end{aligned} \tag{25}$$

Note that $\Phi^{(1)}$ and $\Phi^{(2)}$ are special Green's functions satisfying the conditions $\partial\Phi^{(1)}/\partial x_1=0$ and $\partial\Phi^{(2)}/\partial x_1=0$ on the horizontal edges $x_1=0$ and $x_1=h$ of the representative strip. With such special Green's functions, the boundary conditions in (19) are exactly satisfied by (22) and (23) and the path of integration in the boundary integral equations in (22) and (23) is over only the interface $C$ between $R^{(1)}$ and $R^{(2)}$. No integration over the infinitely long edges of the representative strip is required. Details on how the special Green's functions may be derived by conformal mappings and how the boundary integral equations may be discretized together with the continuity conditions in (21) to solve approximately for the unknown functions $w^{(r)}$ and $p^{(r)}$ on $C$ are given in Ang [11].

Once $w^{(r)}$ and $p^{(r)}$ are known on $C$, the displacement $w^{(r)}$ may be computed at any interior point $(\xi_1,\xi_2)$ in $R^{(r)}$ by using (22) and (23) with $\lambda^{(p)}(\xi_1,\xi_2)=1$. The central difference formula for the first order derivative of a function may then be used to approximate the strains $\varepsilon_{31}^{(\mathrm{in})}$ and $\varepsilon_{32}^{(\mathrm{in})}$ at $(\xi_1,\xi_2)$. More specifically, for $(\xi_1,\xi_2)$ in the interior of $R^{(r)}$, we make the approximations

$$\begin{aligned}2\varepsilon_{31}^{(\mathrm{in})}(\xi_1,\xi_2)&\simeq\frac{w^{(r)}(\xi_1+\delta,\xi_2)-w^{(r)}(\xi_1-\delta,\xi_2)}{2\delta},\\2\varepsilon_{32}^{(\mathrm{in})}(\xi_1,\xi_2)&\simeq\frac{w^{(r)}(\xi_1,\xi_2+\delta)-w^{(r)}(\xi_1,\xi_2-\delta)}{2\delta},\end{aligned} \tag{26}$$

where $\delta$ is a given sufficiently small number.

The average values of both $d^2u/dx^2$ and the jump in the stress $\sigma_{32}$ over a period length of the interface $C$ can be shown to be zero. Consequently, the averaging procedure cannot be used to determine $\mu_s$ in (4) as it leads to indeterminacy. Hence, the strain energy approach is used here to compute $\mu_s$.

From (17), the strain energy in the representative region $0<x_1<h,-\infty<x_2<\infty$, $0<x_3<B$ of the bimaterial with the microscopically sinusoidal interface $C$ is given by

$$\begin{aligned}U^{(\mathrm{micro})}&=\lim_{H\to\infty}\int_0^B\int_{-H}^H\int_0^h\sigma_{3k}\varepsilon_{3k}dx_1dx_2dx_3\\&=2B\Gamma_0^2h\left(\mu^{(1)}+\mu^{(2)}\right)\lim_{H\to\infty}H\\&+2B\int_{-\infty}^{\infty}\int_0^h\mu\left(2\Gamma_0\varepsilon_{31}^{(\mathrm{in})}+\varepsilon_{3k}^{(\mathrm{in})}\varepsilon_{3k}^{(\mathrm{in})}\right)dx_1dx_2.\end{aligned} \tag{27}$$

The corresponding total strain energy in the bimaterial with the flat membrane-like interface governed by (4) is given by

$$U^{(\mathrm{macro})}=2B\lim_{H\to\infty}\int_{-H}^H\int_0^h\mu\Gamma_0^2dx_1dx_2+\frac{B}{2}\int_0^h\Gamma_0(\Sigma_{31}+\Sigma_{13})dx_1. \tag{28}$$

Use of (8) in (28) gives

$$U^{(\mathrm{macro})}=2B\Gamma_0^2h\left(\mu^{(1)}+\mu^{(2)}\right)\lim_{H\to\infty}H+2B\left(\mu_s-\frac{1}{2}\sigma_0\right)\Gamma_0^2h. \tag{29}$$

Taking $U^{(\mathrm{micro})}=U^{(\mathrm{macro})}$, we obtain

$$\mu_s-\frac{1}{2}\sigma_0=\frac{1}{h}\int_{-\infty}^{\infty}\int_0^h\mu\left(2\frac{\varepsilon_{31}^{(\mathrm{in})}}{\Gamma_0}+\frac{\varepsilon_{3k}^{(\mathrm{in})}\varepsilon_{3k}^{(\mathrm{in})}}{\Gamma_0^2}\right)dx_1dx_2. \tag{30}$$

The double integral in (30) may be evaluated numerically by replacing the integration domain $0<x_1<h$, $-\infty<x_2<\infty$, with

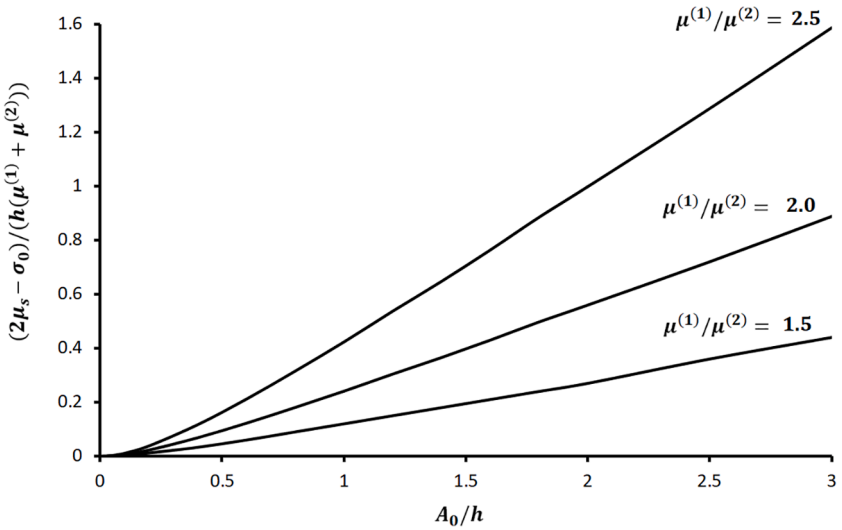


**Fig. 4.** Plots of $(2\mu_s - \sigma_0)/(h(\mu^{(1)} + \mu^{(2)}))$ against $A_0/h$.

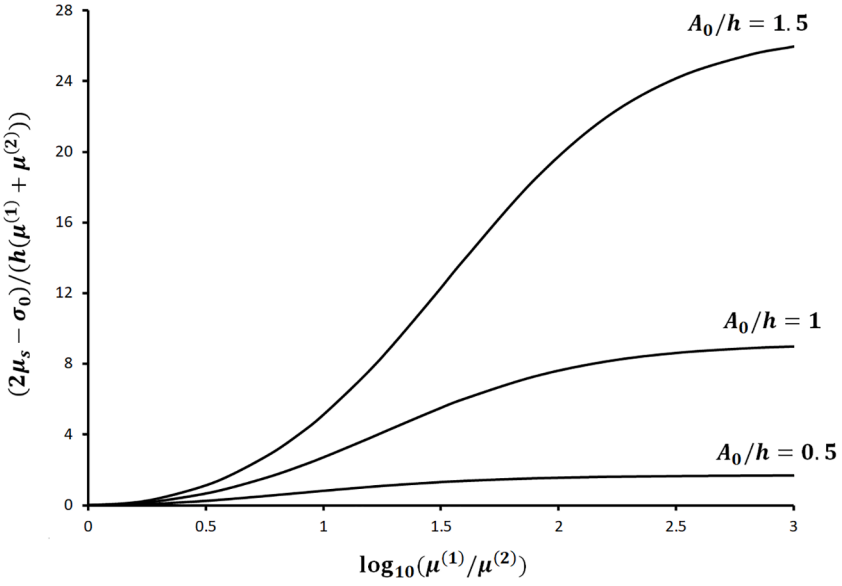


**Fig. 5.** Plots of $(2\mu_s - \sigma_0)/(h(\mu^{(1)} + \mu^{(2)}))$ against $\log_{10}(\mu^{(1)}/\mu^{(2)})$.

$0 < x_1 < h$, $-H < x_2 < H$, where $H$ is a sufficiently large positive real number, and by partitioning the truncated region of integration into many small cells. The strains $\varepsilon_{3k}^{(\text{in})}$ are computed using the approximations in (26).

### 4.3. Results

The non-dimensionalized effective property $(2\mu_s - \sigma_0)/(h(\mu^{(1)} + \mu^{(2)}))$ is a function of only $A_0/h$ and $\mu^{(1)}/\mu^{(2)}$. Furthermore, it has the same value for $\mu^{(1)}/\mu^{(2)} = c$ and $\mu^{(1)}/\mu^{(2)} = 1/c$, where $c$ is a positive constant. In examining the effect of $\mu^{(1)}/\mu^{(2)}$ on $(2\mu_s - \sigma_0)/(h(\mu^{(1)} + \mu^{(2)}))$, one needs to consider only the range given by either $0 \leq \mu^{(1)}/\mu^{(2)} \leq 1$ or $\mu^{(1)}/\mu^{(2)} \geq 1$.

Plots of $(2\mu_s - \sigma_0)/(h(\mu^{(1)} + \mu^{(2)}))$ against $A_0/h$ are given in Fig. 4 for selected values of $\mu^{(1)}/\mu^{(2)}$ greater than 1. For a given $\mu^{(1)}/\mu^{(2)}$, it appears that $(2\mu_s - \sigma_0)/(h(\mu^{(1)} + \mu^{(2)}))$ increases monotonically with $A_0/h$, in an almost linear manner for large $A_0/h$. Also, for $A_0/h = 0$ as well as for $\mu^{(1)}/\mu^{(2)} = 1$, non-dimensionalized effective property $(2\mu_s - \sigma_0)/(h(\mu^{(1)} + \mu^{(2)}))$ is found to be zero, that is, the interface is perfect. This is as expected, as there is no jump in $\sigma_{32}$ across the interface at the microscopic level if $A_0/h = 0$ or $\mu^{(1)}/\mu^{(2)} = 1$. Thus, the interface tends to a perfect one, as $A_0$ approaches zero (for a fixed $h$) or as $h$ becomes increasingly large (for a fixed $A_0$).

From Fig. 4, for a fixed $A_0/h$, it appears that $(2\mu_s - \sigma_0)/(h(\mu^{(1)} + \mu^{(2)}))$ is an increasing function of $\mu^{(1)}/\mu^{(2)}$ for $\mu^{(1)}/\mu^{(2)} \geq 1$. To investigate this further, plots of $(2\mu_s - \sigma_0)/(h(\mu^{(1)} + \mu^{(2)}))$ against $\log_{10}(\mu^{(1)}/\mu^{(2)})$ with $\mu^{(1)}/\mu^{(2)} \geq 1$ are given in Fig. 5 for selected values of $A_0/h$. From the plots, it is observed that $(2\mu_s - \sigma_0)/(h(\mu^{(1)} + \mu^{(2)}))$ increases slowly with increasing $\mu^{(1)}/\mu^{(2)}$. For a given value of $A_0/h$, it appears that $(2\mu_s - \sigma_0)/(h(\mu^{(1)} + \mu^{(2)}))$ approaches a particular value as $\mu^{(1)}/\mu^{(2)}$ tends to infinity. The case of an elastic half space with a traction free microscopically wavy boundary may be recovered by letting $\mu^{(1)}/\mu^{(2)}$ tend to infinity for a fixed value of $\mu^{(1)}$, that is, by letting $\mu^{(2)}$ tend to zero. At the macroscopic level, the traction free wavy boundary is a flat membrane characterized by $\mu_s$ with a finite value.

## 5. Summary

An interface damaged by a periodic array of interfacial micro-cracks and one that has a microscopically sinusoidal profile are modeled as a spring-like and a membrane-like interface respectively at the macroscopic level.

The effective property of the spring-like interface may be computed by using the averaging procedure in Wang et al [6]-[7]. Nevertheless, the averaging approach cannot be extended to calculate the effective property of the membrane-like interface, as it leads to indeterminacy. An energy approach which equates the strain energy in the microscopic model to that in the macroscopic model is used here to estimate the effective property of the spring-like interface as well as that of the membrane-like interface. The two approaches show good agreement in the computation of the effective property of the spring-like interface.

How the effective property of the microscopically wavy interface may be affected by the wavy interface amplitude and the shear moduli of the materials separated by the interface is investigated. The results obtained are intuitively acceptable from a physical point of view.

## Declaration of Competing Interest

The authors declare that they have no known competing financial interests or personal relationships that could have appeared to influence the work reported in this paper.

## References

[1] M.E. Gurtin, A.I. Murdoch, A continuum theory of elastic material surfaces, Arch Ration Mech Anal 57 (1975) 291–323.
[2] M.E. Gurtin, A.I. Murdoch, Surface stress in solids, Int J Solids Struct 14 (1978) 431–440.
[3] Y. Benveniste, T. Miloh, Imperfect soft and stiff interfaces in two-dimensional elasticity, Mech. Mater. 33 (2001) 309–323.
[4] M.E. Gurtin, J. Weissmuller, F. Larche, A general theory of curved deformable interface in solids at equilibrium, Philos. Mag. A 78 (1998) 1093–1109.
[5] H. Fan, K.Y. Sze, A micro-mechanics model for imperfect interface in dielectric materials, Mech. Mater. 33 (2001) 363–370.
[6] X. Wang, W.T. Ang, H. Fan, Micro-mechanics models for an imperfect interface under anti-plane shear load: hypersingular integral formulations, Eng Anal Bound Elem 36 (2012) 1856–1864.
[7] X. Wang, H. Fan, W.T. Ang, On micromechanical-statistical modeling of microscopically damaged interfaces under antiplane deformations, Int J Solids Struct 51 (2014) 2327–2335.
[8] H. Fan, Z.M. Xiao, Dislocation interacting with a slightly wavy interface, Mech. Mater. 23 (1996) 21–28.
[9] W.T. Ang, Hypersingular Integral Equations in Fracture Analysis, Woodhead Publishing, Cambridge, 2013.
[10] A.C. Kaya, F. Erdogan, On the solution of integral equations with strongly singular kernels, Q top Q. Appl. Math. 45 (1987) 105–122.
[11] W.T. Ang, A Beginner's Course in Boundary Element Methods, Universal Publishers, Boca Raton, 2007.